Stem Cell Research 45 (2020) 101761

Contents lists available at ScienceDirect

Stem Cell Research

journal homepage: www.elsevier.com/locate/scr

Characterization and application of electrically active neuronal networks established from human induced pluripotent stem cell-derived neural progenitor cells for neurotoxicity evaluation

Laura Nimtz[a], Julia Hartmann[a], Julia Tigges[a], Stefan Masjosthusmann[a], Martin Schmuck[a], Eike Keßel[a,b], Stephan Theiss[c], Karl Köhrer[d], Patrick Petzsch[d], James Adjaye[e], Claudia Wigmann[a], Dagmar Wieczorek[f], Barbara Hildebrandt[f], Farina Bendt[a], Ulrike Hübenthal[a], Gabriele Brockerhoff[a], Ellen Fritsche[a,g,*]

[a] IUF - Leibniz Research Institute for Environmental Medicine, Duesseldorf, Germany
[b] Department of Biophysics, Ruhr-University Bochum, Bochum, Germany
[c] Medical Faculty, Institute of Clinical Neuroscience and Medical Psychology, Heinrich-Heine-University, Duesseldorf, Germany
[d] Biological and Medical Research Centre (BMFZ), Medical Faculty, Heinrich-Heine-University, Universitätsstraße 1, 40225 Duesseldorf, Germany
[e] Medical Faculty, Institute for Stem Cell Research & Regenerative Medicine, Heinrich-Heine-University, Duesseldorf, Germany
[f] Medical Faculty, Institute of Human Genetics, Heinrich-Heine-University, Duesseldorf, Germany
[g] Medical Faculty, Heinrich-Heine-University, Düsseldorf, Germany

ARTICLE INFO

Keywords:
Neurotoxicology
Stem cell
hiPSC-NPC
MEA
Neuronal network
Electrical activity
Transcriptome
Dopaminergic
Cholinergic
In vitro in vivo comparison

ABSTRACT

Neurotoxicity is mediated by a variety of modes-of-actions leading to disturbance of neuronal function. In order to screen larger numbers of compounds for their neurotoxic potential, *in vitro* functional neuronal networks (NN) might be helpful tools. We established and characterized human NN (hNN) from hiPSC-derived neural progenitor cells by comparing hNN formation with two different differentiation media: in presence (CINDA) and absence (neural differentiation medium (NDM)) of maturation-supporting factors. As a NN control we included differentiating rat NN (rNN) in the study. Gene/protein expression and electrical activity from *in vitro* developing NN were assessed at multiple time points. Transcriptomes of 5, 14 and 28 days *in vitro* CINDA-grown hNN were compared to gene expression profiles of *in vivo* human developing brains. Molecular expression analyses as well as measures of electrical activity indicate that NN mature into neurons of different subtypes and astrocytes over time. In contrast to rNN, hNN are less electrically active within the same period of differentiation time, yet hNN grown in CINDA medium develop higher firing rates than hNN without supplements. Challenge of NN with neuronal receptor stimulators and inhibitors demonstrate presence of inhibitory, GABAergic neurons, whereas glutamatergic responses are limited. hiPSC-derived GABAergic hNN grown in CINDA medium might be a useful tool as part of an *in vitro* battery for assessing neurotoxicity.

1. Introduction

For protecting human and environmental health, industrial, agricultural and consumer products must be registered and approved by the European Food Safety Authority (EFSA) or the European Chemical Agency (ECHA) before entering the market. Neurotoxic effects are of major scientific and socio-political concern, because they often result in irreversible adverse outcomes (Costa et al., 2008; Aschner et al., 2017). Neurotoxicity guideline studies (OECD, 1997; EPA, 1998) are currently performed *in vivo*. These are resource-intensive regarding the time and costs required (Bal-Price et al., 2008) and might not well reflect the human situation because of inter-species variations (Matthews, 2008; Leist and Hartung, 2013). Therefore, alternative *in vitro* testing strategies based on human cells that reduce or replace animal experiments (Russell et al., 1959) are of high interest for neurotoxicity research (Coecke et al., 2006; Zuang et al., 2018). Medium- to high-throughput *in vitro* testing requires a large amount of cell material. In contrast to the use of human embryonic stem cells, which bear ethical concerns (Kao et al., 2008; Singh et al., 2015; Mayer et al., 2018) human induced pluripotent stem cells (hiPSC) are ideal for providing an ethically

* Corresponding author at: IUF - Leibniz Institute for Environmental Medicine, Auf'm Hennekamp 50, 40225 Duesseldorf, Germany.
E-mail address: ellen.fritsche@iuf-duesseldorf.de (E. Fritsche).

https://doi.org/10.1016/j.scr.2020.101761
Received 25 June 2019; Received in revised form 20 February 2020; Accepted 5 March 2020
Available online 10 March 2020

inoffensive and unlimited supply of material for *in vitro* neurotoxicological evaluations (Takahashi et al., 2007; Robinton and Daley, 2012; Zagoura et al., 2017). For screening larger numbers of compounds for their neurotoxic potential, *in vitro* functional neuronal networks (NN) derived from hiPSC might be helpful tools. Neural differentiation, NN formation and establishment of functional signal transmissions for neurotoxicity assessment based on hiPSC is thus very auspicious, yet still barely studied (Odawara et al., 2014; Cotterill et al., 2016; Kasteel and Westerink, 2017; Pistollato et al., 2017; Paavilainen et al., 2018; Tukker et al., 2018; Izsak et al., 2019Hyvärinen et al., 2019), especially in light of the multiple modes-of-actions (MoA) initiating disturbance of neuronal functions (Masjosthusmann et al., 2018a).

One method for studying electrophysiology of neurons and NN is the microelectrode array (MEA) technology. MEAs record extracellular local field potentials at different locations of neurons on a network-level and provide data about their activity properties and patterns (Johnstone et al., 2010). The MEA technology allows assessment of NN electrical activity in real-time and evaluation of the dynamics of network behavior under chemical manipulations (Odawara et al., 2014, 2016; Tukker et al., 2016, 2018). The use of MEAs in toxicological testing is relatively new and has so far been mainly applied for rat NN (rNN) (Hogberg et al., 2011; McConnell et al., 2012; Valdivia et al., 2014; Brown et al., 2016; Cotterill et al., 2016; Frank et al., 2017; Vassallo et al., 2017; Shafer et al., 2019Wagenaar et al., 2006Napoli and Obeid, 2016).

In this study, we continue our previous work on neural induction of hiPSC (Hofrichter et al., 2017) by establishing and characterizing human NN (hNN) from hiPSC-derived neural progenitor cells (hiNPC) by comparing hNN formation with two different differentiation media: in presence (CINDA) and absence (NDM) of maturation-supporting factors. As a NN control we included differentiating rNN. Gene and protein expression and electrical activity from *in vitro* developing NN were assessed at multiple time points and in presence and absence of pharmacological compounds. In addition, microarrays were performed for transcriptome analyses of hNN, which were compared to *in vivo* transcriptomes of human developing brains.

2. Material and methods

2.1. Compounds used

γ-Aminobutyric acid (GABA), Glutamate and Domoic acid (DA) were obtained from Sigma Aldrich (Saint Louis, USA). NBQX disodium salt, DL-AP5 sodium salt and Bicuculline were obtained from Santa Cruz Biotechnologies (Texas, USA). CytoToxOne Cytotoxicity Assay Kit was obtained from Promega Corporation (Madison, USA). For detailed information and solvents see Supplementary Material.

2.2. Cell culture and neural induction

The hiPSC lines A4 (Wang and Adjaye, 2011) and IMR-90 (Clone-4, WiCell,USA) were cultured in mTeSR1 medium (Stemcell Technologies, Germany) on Matrigel (BD Bioscience, Germany). Medium was changed every day and cells were passaged chemically in colonies with 0.5 mM EDTA. hiPSC lines were regularly tested for their pluripotency and their chromosomal integrity.

Neural induction of hiPSC lines was performed using the neural induction medium (NIM) protocol according to (Hofrichter et al., 2017). Briefly, hiPSC colonies were cut in 200 × 200 µm squares using a passaging tool (STEMPRO EZPassage,Thermo Fisher Scientific) and cultured on polyhema (Sigma Aldrich) coated dishes with NIM medium (for detailed medium composition see Supplementary Material) for 7 days. Generated free-floating 3D-Spheres were transferred into new polyhema dishes with NIM containing 10 ng/mL bFGF (R&D Systems, Germany) for another 14 days. Afterwards they were referred to as hiNPC and cultured in polyhema dishes with neural proliferation medium (NPM, see Supplementary Material).

Primary rat NPC (rNPC) were prepared from full brains of Wistar rats on postnatal day 1 as previously described (Baumann et al., 2014). 3D neurospheres were cultured free-floating in NPM and half of the medium was changed every 2–3 days.

Proliferating NPC at a diameter of 400–500 µm were cut into 200 × 200 µm squares using a McIlwaine tissue chopper (Mickle Laboratory, UK) to expand the culture (Fritsche et al., 2011; Baumann et al., 2014). For experimental use, spheres were chopped 2 days before plating.

2.3. Neuronal differentiation and immunocytochemistry

Neuronal differentiation and immunocytochemistry were performed as described previously by Hofrichter et al., 2017, using NDM and CINDA medium, the latter consisting of NDM, **c**reatine monohydrate, **i**nterferon-γ, **n**eurotrophin-3, **d**ibutyryl-cAMP and **a**scorbic acid. For detailed information and medium composition see Supplementary Material.

Quantification of synapses and receptors was performed by analyzing neurite mass in μm^2 and number of synapses (synapses/neurite area (μm^2)) using the Omnisphero software as previously described (Hofrichter et al., 2017). Due to differences in TUBB3 intensities between rat and human cells, different structuring elements were used to eliminate uneven backgrounds. Resulting images were thresholded with the Otsu method (for detailed information see Supplementary Material).

2.4. Quantitative reverse-transcription PCR

RNA was isolated using the RNeasy Mini Kit (Qiagen, Germany) according to manufacturer's protocol. RNA of hiPSC (undifferentiated controls), proliferating hiNPC and rNPC (30 neurospheres of 300 µm diameter each) and human and rat NN after 7, 14, 21 and 28 days *in vitro* (DIV) were prepared. For the latter, cells were chopped to 100 µm aggregates and plated on poly-D-lysine (PDL)/laminin-coated 24-well-plates in NDM or CINDA (hiNPC) or only NDM (rNPC). For reverse transcription, 500 ng RNA was transcribed into cDNA using the QuantiTect Reverse Transcription Kit (Qiagen, Germany). Quantitative polymerase chain reaction (q-RT-PCR) was performed using the QuantiFast SYBR Green PCR Kit (Qiagen, Germany) in the Rotor Gene Q Cycler (Qiagen, Germany) following manufacturer's instructions. Analysis was performed using standards of the gene of interest, allowing to calculate copy numbers, and expression was normalized to β-actin (Dach et al., 2017). Each experiment was performed at least three times with three independent neural inductions. For primer sequences see Supplementary Material.

2.5. NN differentiation on microelectrode arrays (MEA)

Electrical activities of NN were recorded as described in Hofrichter et al., 2017. Briefly, we used 200 hiNPC or rNPC neurospheres (100 µm diameter), seeded onto PDL/laminin pre-coated single-well MEAs (Multichannelsystems (MCS), Germany) either in NDM or CINDA medium. Recordings were performed with the MC-Rack (MCS, Germany) from 2 to 15 weeks *in vitro*. After approximately 5 min of equilibration, each recording consisted of a 5 min baseline recording of spontaneous activity. For data analyses the first minute was cut off and mean values of the mean firing rate (MFR), mean bursting rate (MBR), spikes per burst and active electrodes (AE) of the last 4 min were calculated. For statistical analyses see Supplementary Material.

2.6. NN characterization with pharmaceuticals

To characterize NN regarding their receptor composition MEA chips

were equilibrated in the MEA-headstage 2 min prior to recording. To be regarded as active, NN had to have a minimum of 3 AE. These were defined by the detection of a minimum of 5 spikes/min. For treatment analyses, a baseline measurement of active MEAs for 5 min was recorded. Afterwards, the respective receptor agonist/antagonist was added to the well and allowed to equilibrate for 5 min (wash-in-phase), followed by 5 min recording. Then MEAs were washed twice with medium (wash-out-phase) and further cultivated in fresh medium. Measurements of receptor treatment were performed twice a week starting at day 7. The recordings and data analyses were done as described in 2.5.

2.7. DA treatment on multi-well-MEAs (mwMEAs)

24-well MEA plates (MCS, Germany), each well containing 12 gold electrodes were used. Wells were coated with PDL (0.1 mg/mL, 50 µL for 48 h at 4 °C; Sigma Aldrich) washed with PBS and coated with Laminin (0.01 mg/mL, 48 h at 4 °C, L2020, Sigma Aldrich). Afterwards, 50 hiNPC or rNPC spheres (100 µm diameter) were seeded into the wells and incubated with NDM or CINDA medium, respectively. MwMEAs were recorded with the Multiwell-Screen (MCS) and analyzed with Multiwell-Analyzer (MCS, Germany). For details on hardware settings and spike and burst detection parameters see Supplementary Material. Active networks were defined as stated in 2.5. Individual recordings were performed in week 2–6, in the absence (baseline) and presence of the indicated concentrations of DA in NDM or CINDA for 15 min.

2.8. Affymetrix microarrays

For hiPSC and hiNPC (30 neurospheres of 300 µm diameter each) isolation of RNA was performed using the RNeasy Mini Kit (Qiagen, Germany) according to manufacturer's protocol. Therefore, cells were chopped to 100 µm aggregates and plated on PDL/laminin-coated 6-well-plates. After 5, 14 and 28 days of cultivation in CINDA medium cells were harvested and RNA was isolated. cDNA synthesis and biotin labeling of cDNA was performed according to the manufacturer's protocol (3´ IVT Plus Kit; Affymetrix, Inc.) and as previously described (Masjostusmann et al., 2018b). For detailed information on the gene expression analysis by microarrays see Supplementary Material.

2.9. Data analysis and statistics

Unless otherwise stated all statistical analyses were performed using GraphPad Prism 6.00 for Windows (GraphPad, USA). Immunocytochemical quantification and pharmaceutical data were analyzed using one-way ANOVA, qRT-PCR and DA-treatment data were analyzed using a two-way ANOVA followed by a Bonferroni test to correct for multiple testing. The significance cut-off was set to $p \leq 0.05$.

3. Results

3.1. Molecular characterization of hiNPC-differentiated cultures

Differentiation of hiNPC was performed with NDM and maturation supporting CINDA medium. Before plating, hiNPC stained positive for the markers PAX6, NESTIN and SOX2 (Fig. S1). After 28DIV hiNPC grown in NDM or CINDA medium and rNPC grown in NDM differentiated into TUBB3$^+$ neurons and GFAP$^+$ astrocytes (Figs. 1 and 2A; Fig. S2). Human neurons express the pre- and postsynaptic proteins SYN1 and PSD95 as well as the receptor-specific proteins GABAARβ, GluR1 and NMDAR1 with no significant differences between the tested medium conditions, *i.e.* NDM and CINDA (Fig. 2A and B). To further characterize the networks, mRNA expression analyses were performed and gene copy numbers determined by product-specific standards. This procedure enables comparison of gene expression across species and has the advantage of giving information on magnitude of absolute gene expression rather than relative gene changes as by using the ΔΔCT method (Gassmann et al., 2010; Walter et al., 2019). Gene expression of the NPC marker *NESTIN* was stably expressed in human cultures over time, whereas its expression significantly decreased in rat cultures starting at DIV14 (Fig. 3A). The expression of the mature astrocyte marker *AQP4* was significantly upregulated on DIV28 in CINDA- compared to NDM-cultures, whereas *Aqp4* expression in rat cultures increased early starting at DIV7 (Fig. 3C). Expression of the glial fibrillar astrocytic protein *gfap/GFAP* significantly increased from DIV7 in rNN but exhibited only marginal changes in human cells (Fig. 3D). The neuronal marker *MAP2* increased in hNN from DIV7 and low expression values for *map2* were observed in rNN (Fig. 3E). To analyze the time of synapse formation we used the pre- and post-synaptic markers *SYN1* and *DLG4,* respectively, which are expressed after 7DIV in both species (Fig. 3F–G). Expression of *SLC17A7* (glutamate transporter vGLUT1) and *GAD1* (glutamic acid decarboxylase) differ remarkably. While *SLC17A7* copy numbers are extremely low (<1–5 copy numbers/10,000 copies *β-ACTIN*), *GAD1* is well expressed (>100 copy numbers/10,000 copies *β-ACTIN*) suggesting predominantly GABAergic neurotransmission (Fig. 3H and I). Concerning neuronal subtypes, hNN show an increasing expression of *ACHE* (acetylcholinesterase), *GRIA1* (AMPA receptor), and *TH* (tyrosine hydroxylase) over time with *TH* expression being significantly induced on 14DIV in CINDA-NN compared to NDM-NN (Fig. 3J), while similar to *SLC17A7, GRIN1* (NMDAR, Fig. 3K) and *SLC6A4 (*serotonergic neurons*,* Fig. S3*)* copy numbers are very low. In contrast, rNN revealed very low expression of *ache* and *th* (<1 copy numbers/10,000 copies *β-actin*) compared to human cells (Fig. 3J and M).

3.2. Electrical activity of hiNPC–CINDA- and hiNPC–NDM-NN over time

We studied whether differentiation of neural cultures resulted in generation of functional NN. Therefore, we examined multiple electrophysiological parameters on MEA chips for single electrodes as well as the entire network. Human NN exhibited spontaneous electrical activity after 2 weeks in culture. Starting with the same number of MEA-chips for both medium conditions, hNN grown in CINDA medium (CINDA-NN) produced more active chips (Fig. 4; Fig. S4) and higher electrical activities measured as MBR, spikes per burst and the number of AEs than NDM-NN (Fig. 4B–D). In week 3 the mean value of all recorded activities (except for the MFR) was significantly higher in CINDA-NN compared to NDM-NN. NN generated from rNPC serve as positive controls (Mack et al., 2014; Alloisio et al., 2015; Wallace et al., 2015) and displayed higher bursting activity levels than hNN (Fig. 4A–D). Over the entire differentiation time of 15 weeks (Fig. S4), CINDA- and NDM-NN reached highest activity levels of all measured parameters within the first 6 weeks with CINDA-NN exhibiting higher MBR, spikes/burst and number of AEs than NDM-NN. In contrast, rNN reached their maximum activity across all parameters measured within 7 to 11 weeks of differentiation.

3.3. Characterization of NNs with agonists and antagonists of neuronal receptors

To study if differentiated NN contain functional GABAergic and glutamatergic neurons, we treated NN with the GABA receptor (GABAR) agonist GABA or the glutamate receptor agonist glutamate (Fig. 5). NN of both species responded to GABA with a reduction in MFR, MBR and number of spikes/burst (Fig. 5A–C and D) suggesting presence of functional GABARs. Glutamate also decreased these parameters, yet to a lower extent indicating no functional excitatory glutamatergic receptors. Treatment of NN with the GABAR inhibitor bicuculline also reduced MFR and spikes/burst in NN not treated with external GABA (Fig. 5A, C, and E) implying a minimal presence of glutamatergic neurons in the networks. If the NN consisted of a

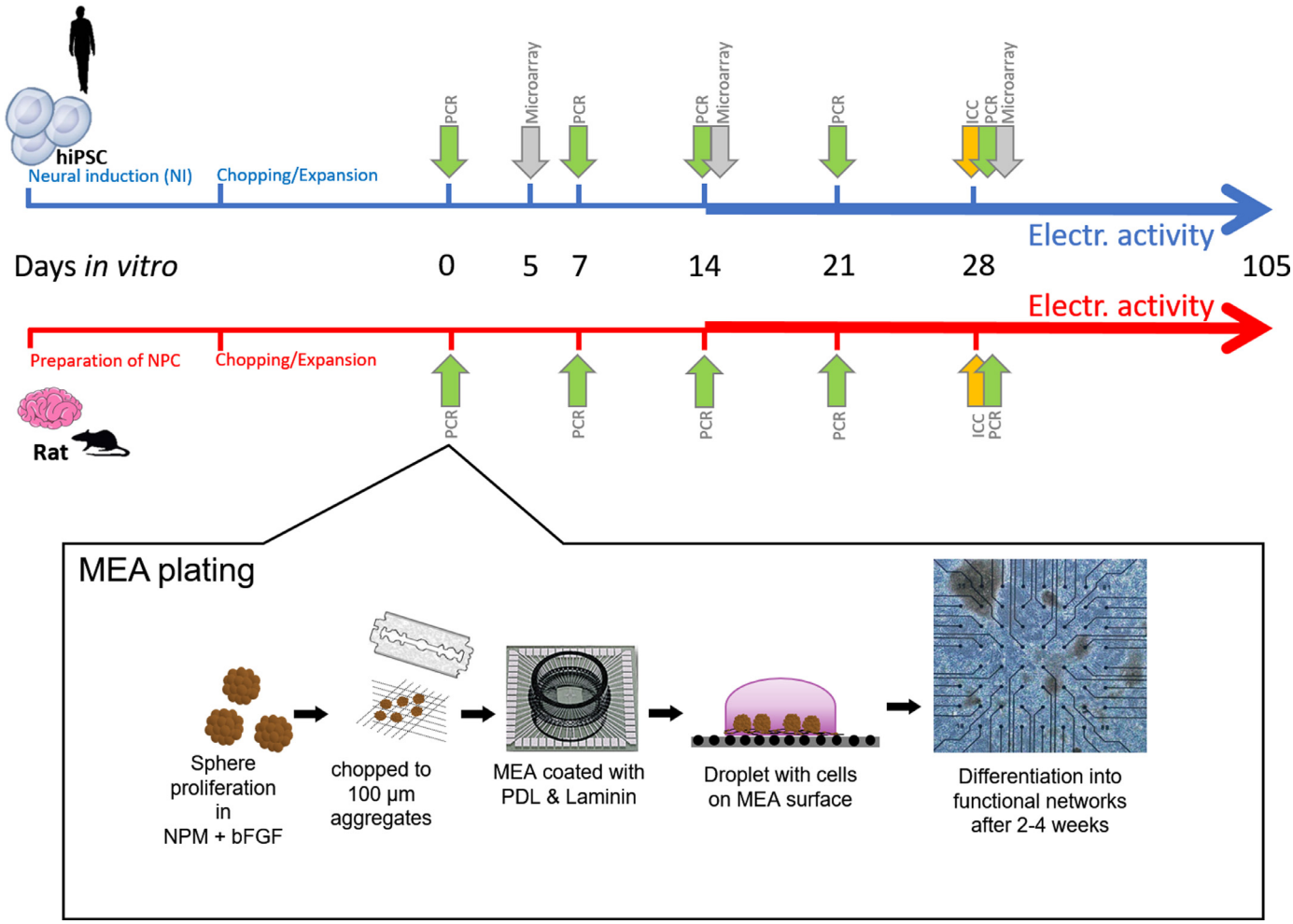

Fig. 1. Experimental set up. hiNPC were neurally induced from hiPSC or generated from rat brain (PND1) and cultivated as floating neurospheres. qRT-PCR analyses and MEA recordings were performed weekly from day 0 until 15 weeks *in vitro*. Cells were fixed for immunocytochemical staining after 28 days of differentiation. For MEA plating spheres were cut into 0.1 mm aggregates and 200 were seeded on PDL/laminin pre-coated MEA recording fields.

comparable amount of glutamatergic and GABAergic neurons, one would expect a strong increase in network activity after bicuculline exposure (Xiang et al., 2007; Mack et al., 2014) that we did not observe. In addition, the NMDAR and AMPAR antagonists, AP5 and NBQX, respectively, exhibited no effects on NN except for AP5 reducing spike frequency in the rNN which suggests the possible presence of NMDAR in rNN (Fig. 5A).

3.4. NN response to the shellfish toxin DA

To determine if the NN assay based on hiNPC differentiated in CINDA medium is a useful tool for acute neurotoxicity testing *in vitro*, we treated CINDA- as well as rNN with the shellfish toxin and glutamate analogue DA (Chandrasekaran et al., 2004; Watanabe et al., 2011; Vassallo et al., 2017), which is a model compound previously used in a multi-laboratory evaluation of MEA-based measurements of neural network activity for acute neurotoxicity testing (Vassallo et al., 2017). DA is an excitotoxicant which binds to postsynaptic glutamate receptors with a 100-fold higher affinity than glutamate, causing receptor overactivation, which leads to neuronal excitotoxicity, neuronal degeneration and ultimately cell death (Watanabe et al., 2011; Magdalini et al., 2019). For concentration-response analyses we used 24-well multiwell-MEAs (mwMEAs) instead of single-well MEAs as a medium throughput setup for compound testing. One well of a mwMEA contains 12 electrodes, compared to 59 electrodes in a single well MEA (Fig 6A). The distances between electrodes are 200 µm. Of the total of 72 and 96 wells measured with human and rat NN, respectively, 33 (45.8%) and 32 wells (44.5%) had 9–12 AE/well, 22 (30.6%) and 30 wells (31.3%) had 5–8 AE/well, 13 (18.1%) and 28 wells (29.2%) had 1–4 AE/well, and only 4 (5.6%) and 6 wells (6.3%) had no AE/well (Fig. 6B). Acute exposure to increasing concentrations of DA for 15 min increased spontaneous activity of hNN and rNN with significant effects only for the total burst count in rNN (Fig. 6C) but did not cause cytotoxicity in either of the networks up to 24 h after exposure (Fig. S5). Although not statistically quantifiable, the firing pattern visualized in the representative Spike Raster Plots (SRP) reveals changes in activity pattern in both species after treatment with 1 µM DA compared to baseline activity (Fig. 6D). Additional activity parameters exhibited no significant changes (Fig. S5).

3.5. Microarray analyses of CINDA-NN and a comparison to published in vivo data

To monitor differentiation and maturation processes of hNN on the transcriptome level, we analyzed mRNA expression profiles of hiPSC, proliferating hiNPC, and hiNPC-derived NN differentiated for 5, 14, and 28DIV in CINDA medium using Human PrimeViewArrays from Affymetrix. Microarray data was validated by qRT-PCR analyses for representative genes (Fig. S6). Only genes that were at least 2-fold significantly regulated ($p \leq 0.05$) were used for subsequent analyses.

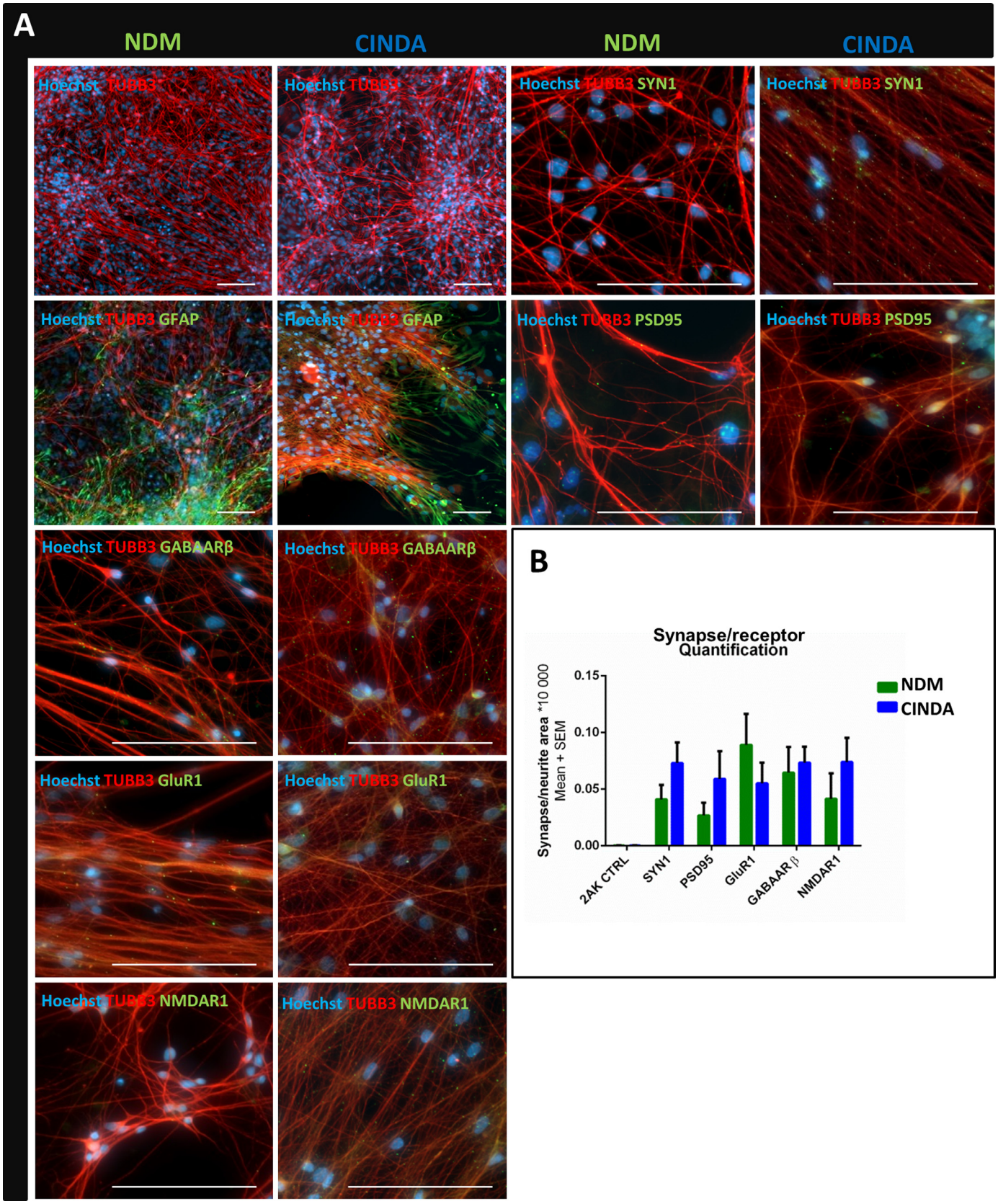

Fig. 2. Immunocytochemical staining of hNN. (A) Representative pictures of hNN differentiated with NDM or CINDA medium for 28 days: neurons (TUBB3; red), astrocytes (GFAP; green), pre- (SYN1) and post synapses (PSD95; green dots), GABA receptor (GABAARβ), glutamate receptor (GLUR1) and NMDA receptor (NMDAR1; green dots). Nuclei were stained with Hoechst. Scale bars are 100 μm. B) Quantifications of synapses/receptors (mean + SEM) as ratio to total neurite area (n = 3–6). (For interpretation of the references to color in this figure legend, the reader is referred to the web version of this article.)

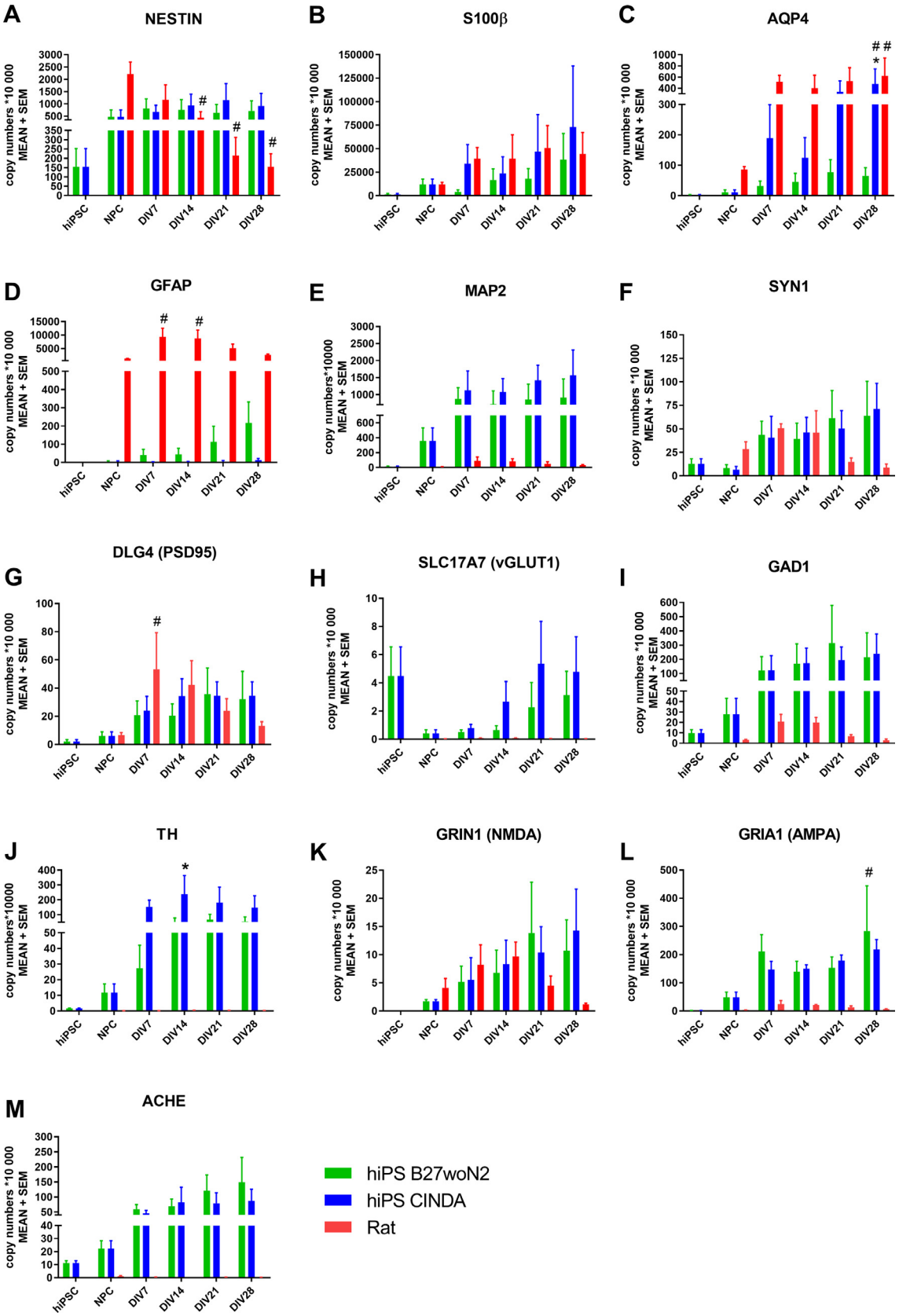

Fig. 3. mRNA expression profiles of hiPSC, hiNPC and hNN compared to rNPC and rNN. qRT-PCR analysis of different cell types for neural progenitor (*NESTIN, MAP2*), astrocyte (*S100β, AQP4, GFAP*), synaptic (*SYN1, DLG4*) and neuronal subtype specific markers (*SLC17A7, ACHE, GRIA1, GRIN1, GAD1, TH*) differentiated for 28 DIV in NDM or CINDA medium. rNN serve as positive control. Data are presented as mean + SEM. *significant to NDM, #significant to NPC ($n = 3$, $p < 0.05$).

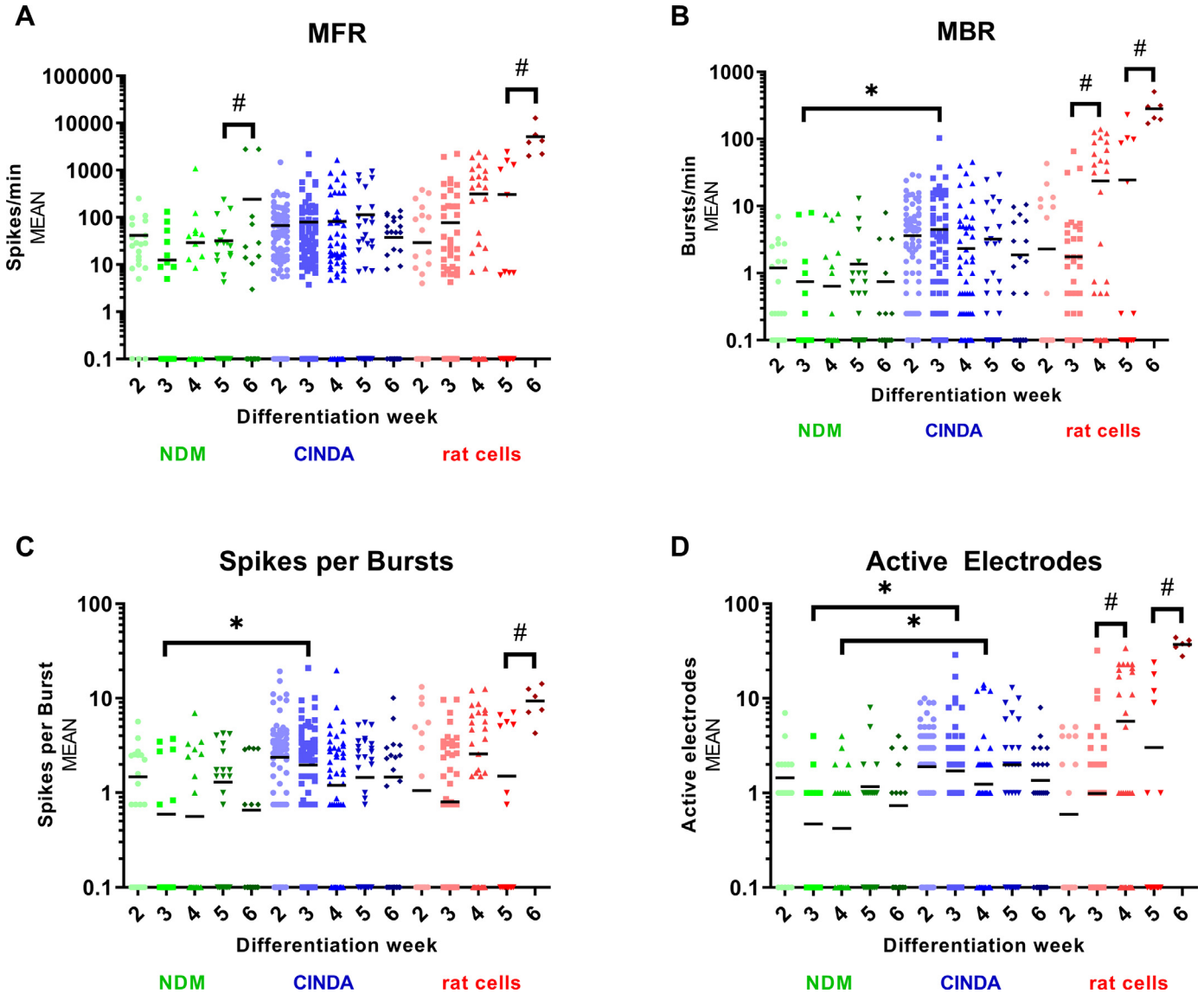

Fig. 4. Spontaneous electrical activity of hNN- and rNN on MEA. Scatter plots of hNN (NDM/CINDA) and rNN differentiated for six weeks on MEAs. Plotted are the (A) MFR, (B) MBR, (C) spikes per burst and (D) AEs, one dot represents the mean of one chip. Both hiNPC: $n = 40$ and rat: $n = 43$ at start of experiment. Black lines represent the mean of all data points. *Significant to NDM, #significant within condition ($p < 0.05$). Note: For a better visualization all values between 0 and 0.1 were manually set to 0.1 so that the data points appear on the X-axis.

Cluster- and principle component analyses (PCA) support the strong differentiation potential of hiPSC (turquoise) into proliferating hiNPC (green) and further neutrally differentiated hiNPC at DIV5 (blue), DIV14 (red) and DIV28 (purple) with very small replicate variations (Fig. 7A and B). In differentiating hiNPC a total of 2629 genes are differentially expressed (DEX) across the three time points (Fig. 7C). The number of DEX genes increased over differentiation time, from 1370 (DIV5) to 1793 (DIV14) and to 2368 (DIV28). The overlap of all conditions was 43.3% (1139 genes), indicating that these genes might be generally important during the transition from a proliferative neural progenitor cell to neural effector cells. This is supported by an over-representation of gene ontology (GO) biological processes related to cell proliferation (*e.g.* GO:0007049~cell cycle, GO:0000280~nuclear division or GO:0006260~DNA replication). In contrast, genes that are regulated between 5 and 14, 14 and 28 as well as 5 and 28 days, control processes related to neuronal differentiation and maturation (e.g. GO:0007399 ~ nervous system development, GO:0048699 ~ generation of neurons, GO:0099537 ~ trans-synaptic signaling; Appendix I). Overrepresentation analysis of GO biological processes of all regulated genes (2629) summarize gene changes of proliferation-differentiation transition as well as neural differentiation and neuronal network maturation (Appendix II). These findings support the *in vitro* development of hNN consisting of neurons and astroglia cells, forming synapses to build a functional NN. To determine to which extent the gene changes observed *in vitro* are representative of the developing human brain *in vivo, in vitro* DEX genes (0vs28DIV) were compared to published DEX genes of *in vivo* transcription profiles of the prefrontal cortex between post-conceptional week 6 (embryonic) and 12 (fetal; (Kang et al., 2011)). These timepoints were chosen based on a recent publication mapping developing brain organoids to *in vivo* fetal brain samples (Amiri et al., 2018). The comparison of *in vivo vs. in vitro* DEX genes revealed that from more than 2837 *in vivo* DEX genes, 868 (44.1% *in vivo* and 36.7% *in vitro*) are commonly regulated (Fig. 7D). DEX gene groups over-represented in these data sets were identified by an over-representation analysis (Appendix III). DEX genes within a selection of manually selected GO-terms including the neural/neuronal specific terms, *i.e.* neural proliferation (NP), astrocytic-, general glia cell- and neuronal differentiation, synapse formation/plasticity, glutamatergic

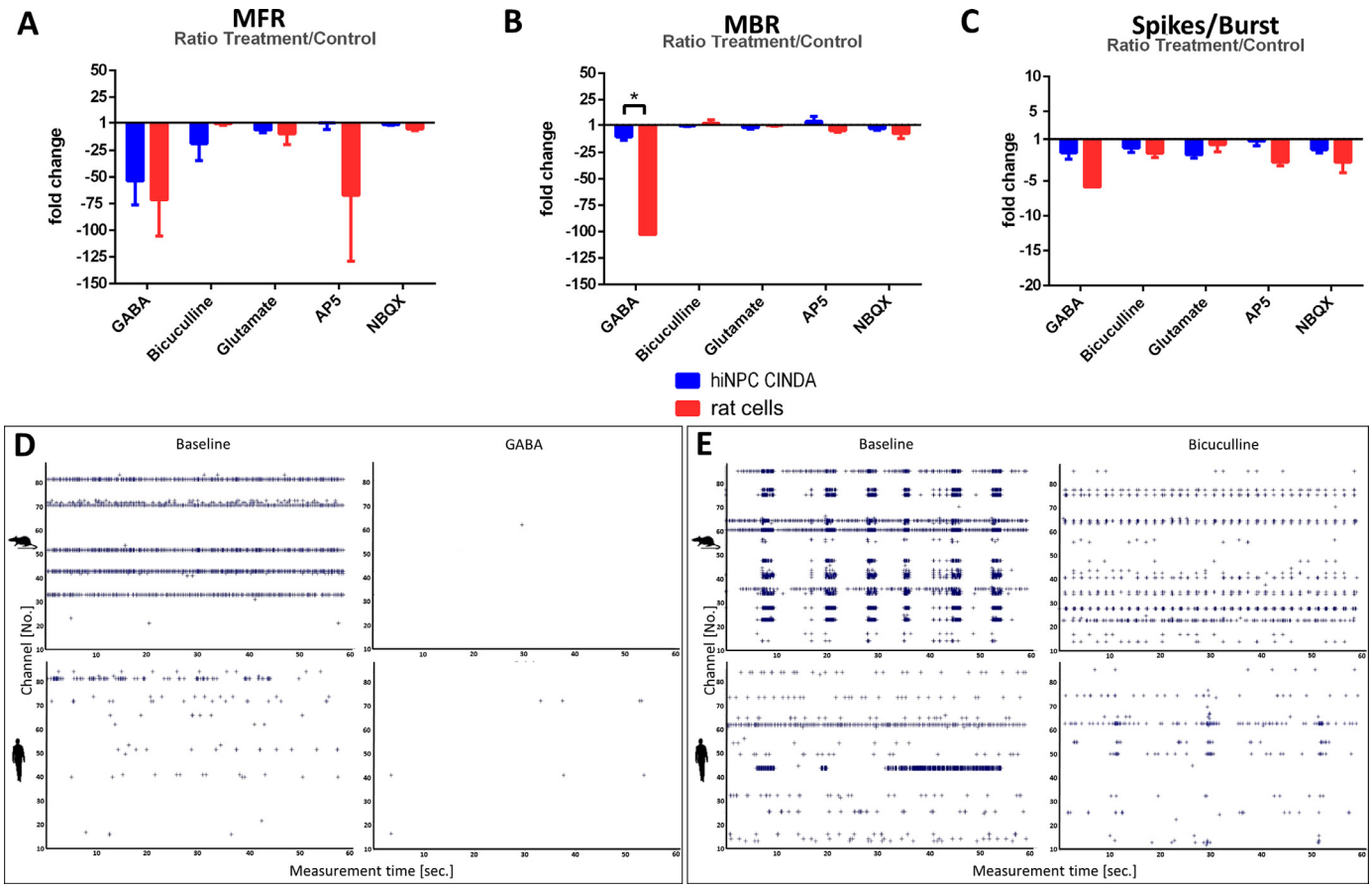

Fig. 5. Modifications of electrical activity by acute pharmacological treatment. Ratio of treatment/control of CINDA-NN and rNN treated with GABA [1 mM], bicuculline [10 μM], glutamate [100 μM], AP5 [20 μM] and NBQX [10 μM]. Results are depicted as A) MFR, B) MBR and C) Spikes/Burst as mean + SEM. hiNPC: $n = 7–10$, rNN: $n = 6–10$. D and E Representative 60 s SRP of hNN and rNN of baseline- and GABA (D) or bicuculline treatment (E). *Significant within condition ($p < 0.05$).

neurons, GABAergic neurons, and radial glia (RG) differentiation (Appendix III) were compared between the *in vitro* and *in vivo* data sets. The result indicates that *in vivo* more GO-terms are enriched, more genes are generally regulated in each GO term and respective genes are mostly stronger regulated *in vivo* than *in vitro,* yet transcriptomes of the *in vitro* cultures reveal well-defined cellular differentiation processes (Fig. 7E, Appendices II and III).

4. Discussion

Human hazard and risk assessment of potentially neurotoxic chemicals is based on *in vivo* animal experiments (Bal-Price et al., 2008). Those experiments are time and cost intensive and do not necessarily reflect the human situation because of inter-species variations (Leist and Hartung, 2013). Thus, alternative *in vitro* testing strategies using human-based material are of special interest for neurotoxicity testing (Coecke et al., 2006; Zuang et al., 2017). We previously established the neural induction of hiPSC to hiNPC, cultured as 3D neurospheres (Hofrichter et al., 2017) and now continued the work by characterizing differentiating hiNPC for their ability of NN formation. We composed the CINDA medium by adding agents to NDM, which support (i) synapse formation, (ii) maturation of different neuronal subtypes and (iii) spontaneous NN activity (Andres et al., 2008; Belinsky et al., 2013; Dutta et al., 2015; Leipzig et al., 2010; Zhu et al., 2012). Human cultures that differentiate over a time course of 28DIV into neurons and astrocytes express *NESTIN* during the whole differentiation time. Although NESTIN is down-regulated and replaced by neurofilaments and *GFAP* during neuro- or gliogenesis *in vivo* (Michalczyk and Ziman, 2005), as well as in the differentiating rat cultures, it was reported by others that neurally differentiated hiNPC do not down-regulate *NESTIN* over time (Pistollato et al., 2014; Zagoura et al., 2017). In human stem cell-derived culture neurogenesis occurs before astrogenesis (Nat et al., 2007; Liu and Zhang, 2011; Yuan et al., 2011). Thus, the neuronal marker *MAP2* already plateaus after 7DIV with no differences between CINDA medium and NDM, while it takes until 21DIV for the astrocyte marker *AQP4* to reach maximum expression. CINDA-NN seem to favor astrocyte differentiation compared to NDM-NN as *AQP4* is significantly higher expressed in CINDA-NN compared to NDM-NN. In contrast, *gfap* expression already levels after 7DIV in rNN followed by a continuous up-regulation of *map2* over the 28DIV. rNN are not produced from iPSC-derived NPC, but are primary NPC prepared from rat postnatal day (PND) 1 pups. These resemble a later developmental phase which might explain the differences in timing (Baumann et al., 2014, Baumann et al., 2016, Masjosthusmann et al., 2018a). Compared to the rat, human NDM-NN express 25–100-fold less *GFAP* and CINDA-NN express little *GFAP* on mRNA level, however, the immunostaining suggests the presence of GFAP protein. One reason for this could be that astrocytes in hNN are protoplasmic, which express far less GFAP than fibrous astrocytes (Molofsky et al., 2012; Molofsky and Deneen, 2015). The significantly stronger *gfap* expression in rNN is likely due to the presence of radial glia in these cultures as suggested by their morphology. Molecular analyses reveal the presence of pre- (*SYN1*) and post-synaptic (*DLG4*/PSD95) structures as well as glutamate NMDA and AMPA receptors and the GABAA receptor in developing NN with no differences between NDM and CINDA medium. Despite receptor expression, glutamatergic

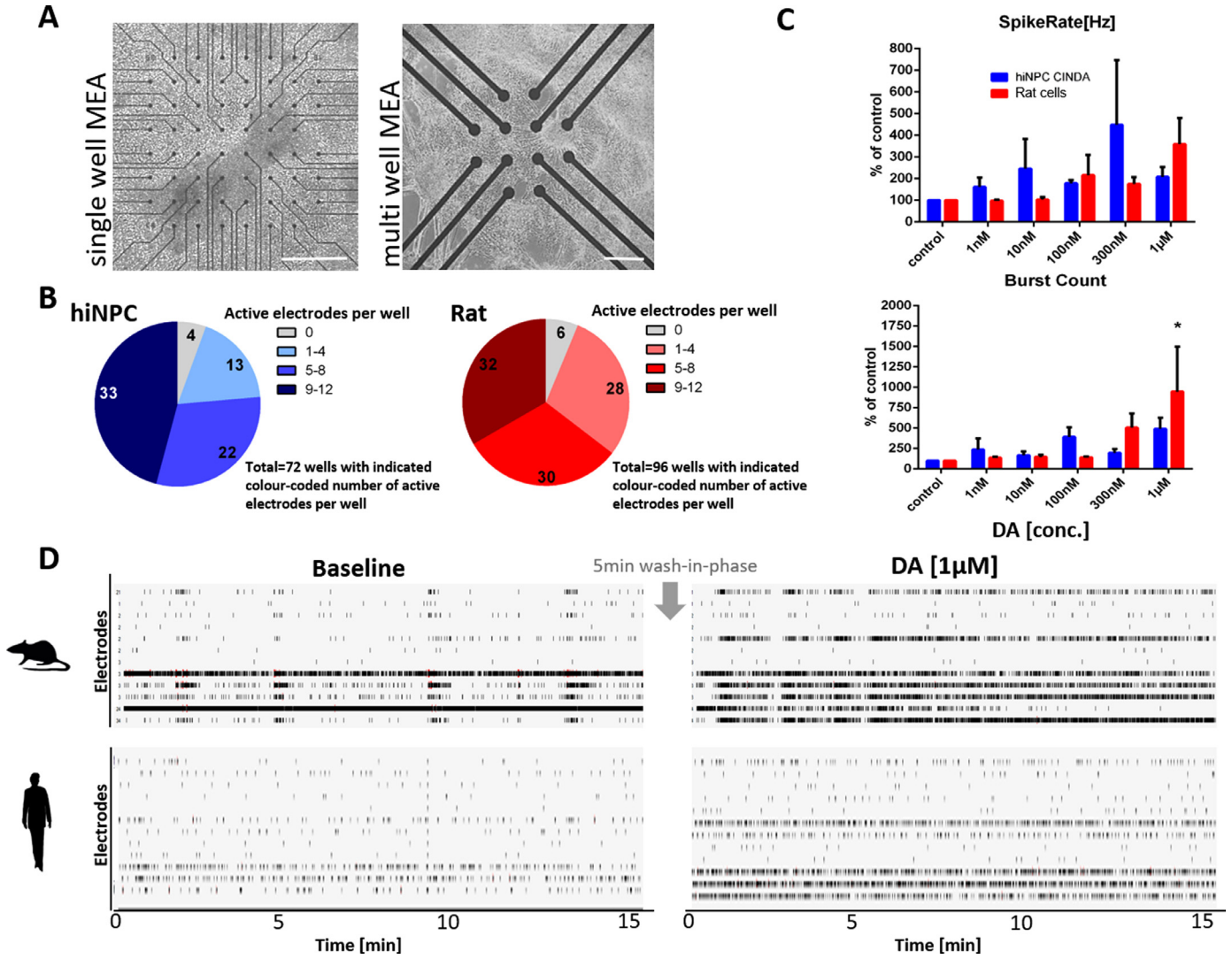

Fig. 6. Acute treatment of NN in mwMEAs with the shellfish toxin DA. (A) Representative phase-contrast images of hiNN on a singlewell- and multiwell-MEA recording field. (B) Pie-diagram of the all wells of hiNN (blue, 72 wells, measured on day 18, 20 and 22) and rNN (red, 96 wells, measured on day 20 and 22) with indication (color-code) of the numbers of AEs per well. (C) Acute treatment of hiNPC and rNN with DA. Mean + SEM of the spike rate [Hz] and the burst count (number of total bursts) are plotted in percent of solvent control for the acute exposure time of 15 min. *significant to control ($n = 3, p < 0.05$). (D) Representative 15 min SRP of 1 µM DA of rNN and hiNN. (For interpretation of the references to color in this figure legend, the reader is referred to the web version of this article.)

neurons seem to be absent in the cultures and neurons mainly seem to be of GABAergic nature with presence of dopaminergic and cholinergic neurons. Here, only *TH* expression was significantly higher expressed in CINDA-NN on DIV14 compared to NDM-NN. Dopaminergic differentiation might be promoted by cAMP in the CINDA medium (Belinsky et al., 2013).

Only few groups have been analyzing electrical activity of hiPSC-derived neural cultures on MEAs (Toivonen et al., 2013; Odawara et al., 2014, 2016; Tukker et al., 2016; Hofrichter et al., 2017; Seidel et al., 2017; Tukker et al., 2018; Izsak et al., 2019; Shimba et al., 2019). Some studied spontaneous firing in hiPSC-derived pure neuronal cultures (Toivonen et al., 2013) or in co-cultures with human (Tukker et al., 2016, 2018) or rat astrocytes (Odawara et al., 2014; Seidel et al., 2017). Astrocytes support neuronal function like signal transmission and maturation, their presence should therefore be advantageous *in vitro* NN (Clarke and Barres, 2013). However, when studying hNN, the use of human instead of rat astrocytes is preferable (Oberheim et al., 2006; Tjarnlund-Wolf et al., 2014). The differentiation protocol used in this study yields hiPSC-derived neurons and astrocytes simultaneously. NN differentiated in two different media, CINDA or NDM, lead to astrocyte maturation and overall electrical network activity with a higher number of AE, MBR and spikes/burst when cells were grown in CINDA medium. Bursting activity is associated with enhanced synapse formation and long-term potentiation of neuronal connections (Maeda et al., 1995; Lisman, 1997) indicating a certain degree of network maturity. rNN were more mature than hNN during week 2–6, indicated by the higher burst activities, possibly due to a faster development of this species (Semple et al., 2013).

To test the functionality of neuronal receptors, we treated hNN, grown in CINDA, and rNN with GABA or glutamate receptor agonists and antagonists. Network data indicates presence of functionally active GABAR that respond to GABA with NN inhibition in both species. In contrast, glutamate receptors seem to be non-functional, as the excitatory neurotransmitter glutamate did not increase spike frequency. The small decrease in MFR upon glutamate treatment might be due to astrocytic glutamate metabolism (Gegelashvili and Schousboe, 1998) to glutamine that is then synthesized to GABA by GABAergic neurons in the absence of glutamatergic neurons (Lujan et al., 2005; Walls et al., 2015). That glutamatergic neurons are non-functional is further supported by a bicuculline treatment: As GABAR inhibitor, bicuculline should increase the NN activity (Fukushima et al., 2016; Odawara et al., 2014, 2016), which is not observed in this study. Very low mRNA

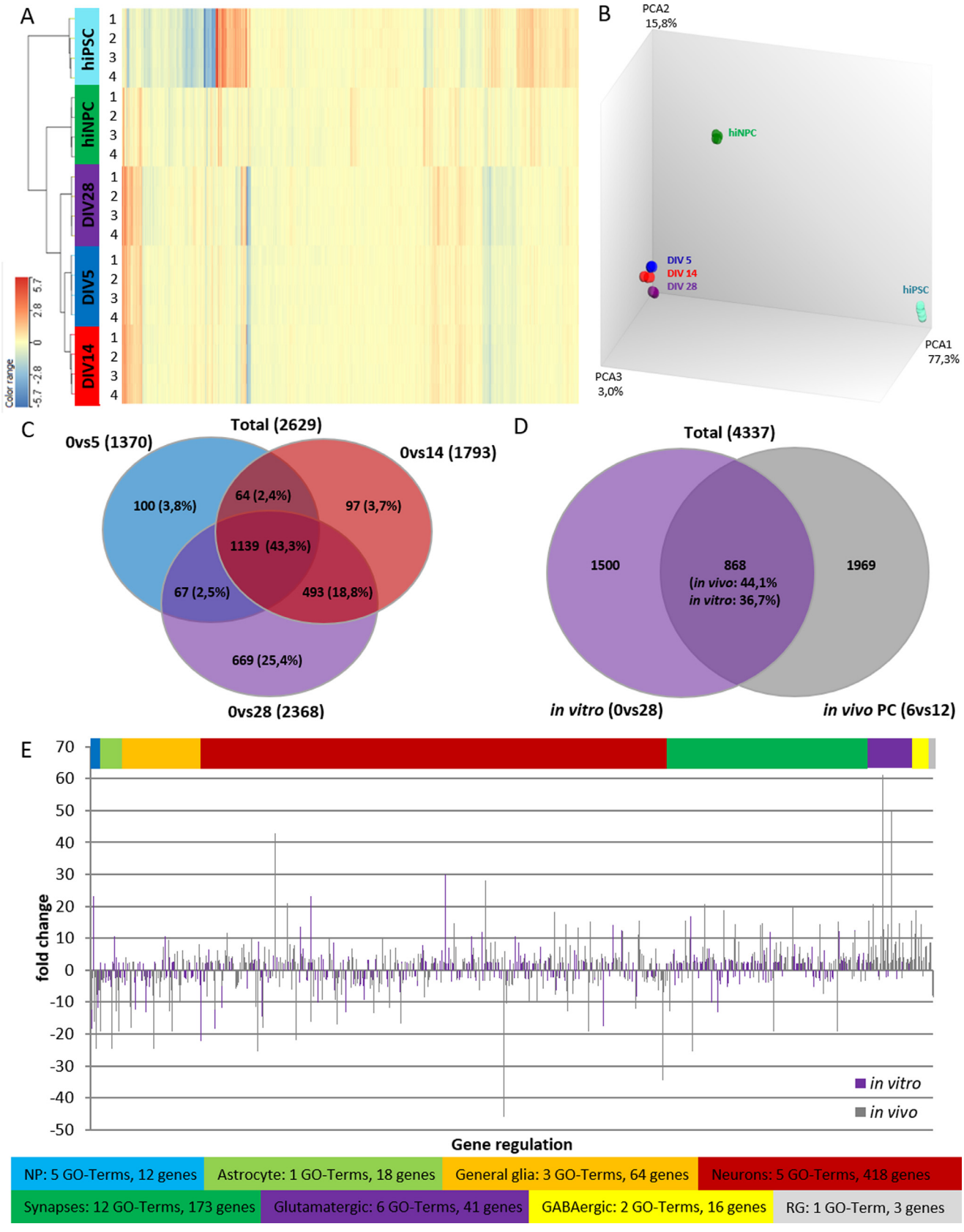

(caption on next page)

expression of *SLC17A7* (vGLUT1) supports these functional findings. Antagonization of the glutamate receptors NMDA and AMPA with AP5 and NBQX, respectively, cause only small changes in hNN activity levels. Presence of their gene products *GRIN1* and *GRIA1* as well as their receptor proteins in combination with the functional data is indicative of not fully matured glutamate receptors. Similar results were

Fig. 7. Transcriptome analyses of hiPSC, hiNPC and hNN and overrepresentation analyses of GO biological processes compared to *in vivo* data. (A) Cluster analysis of hiPSC, hiNPC and hNN. Turquoise = hiPSCs; green = hiNPC; blue = hiNN (DIV5); red = hiNN (DIV14); violet = hiNN (DIV28), 4 replicates each. In the heatmap blue genes are down-regulated, red genes are upregulated. The intensity of the colors serves as a measure of the strength of the regulation ($p \leq 0.05$). (B) PCA of gene expression as demonstrated in (A). (C) Venn-diagram of regulated genes. Plotted are all genes that are significantly ($p \leq 0.05$) up or down regulated by at least 2-fold between the following conditions: red = 0vs5DIV, blue = 0vs14DIV and green = 0vs28DIV. (D) Venn-diagram of regulated genes comparing *in vitro* to *in vivo*. Plotted are all genes that are significantly ($p \leq 0.05$) up or down regulated by at least 2-fold between the following conditions: violet: *in vitro* hiNPC (0vs28DIV) and gray: *in vivo* samples of human prefrontal cortex from week 6vs12 (Kang et al., 2011). (E) Comparative analyses of single gene expression (genes from (D)) annotated to the color-coded GO-terms, which are associated to neural and synaptic markers *in vitro* (violet, 0vs28DIV) and *in vivo* (gray, prefrontal cortex, week 6vs12, (Kang et al., 2011)). (For interpretation of the references to color in this figure legend, the reader is referred to the web version of this article.)

reported from Tang et al., 2013. Plating hiPSC-derived NPCs on laminin for patch-clamp analyses revealed much larger GABA receptor currents than glutamate receptor currents, while NMDA receptor currents were very low in the examined time span of 60DIV. This was similar to previous findings in rat embryonic neurons (Deng et al., 2007) making the authors suggest an evolutionarily conserved role of GABA during early neural development (Tang et al., 2013). However, rNN, which resemble a later developmental stage compared to hNN, seem to possess some functional NMDAR, as addition of AP5 strongly decreases network activity. In the future, the differentiation of hiNPC into also glutamatergic neurons might be achieved by addition of the neurotrophic factors BDNF and GDNF (Izsak et al., 2019) or retinoic acid (Zhang et al., 2013) to the CINDA medium.

It has been proposed that iPSC-derived cell models might be suitable alternative models for future *in vitro* toxicological testings (Jennings, 2015; Suter-Dick et al., 2015). Therefore, we adapted the NN to a 24-well plate MEA testing format that allows higher throughput testing than single well MEAs. Our data suggests that stability and reproducibility of the multi-well MEAs is higher compared to single well MEAs because the number of active chips and the percentage of AE is higher in multi-well compared to single well MEAs. We used the shellfish-toxin DA as a model compound for acute neurotoxicity testing (Vassalo et al., 2017), which causes neuronal excitotoxicity, neuronal degeneration and ultimately cell death (Magdalini et al., 2019; Watanabe et al., 2011). SRP of both analyzed species indicate pattern changes after acute DA exposure, yet only rNN display a significant alteration of the total burst count at 1 μM. NN characterization suggests an immature hNN glutamate receptor system, while rNN seem to possess at least some functional NMDAR that probably mediate the DA effect on the burst count. In previous studies rNN from cortical cultures responded to an acute treatment of 500 nM DA with a decrease of network activity parameters (Hogberg et al., 2011; Wallace et al., 2015; Vassallo et al., 2017), suggesting cytotoxicity of neurons due to hyperstimulation. The higher sensitivity of these cultures is probably due to a higher maturity of primary rat neurons compared to rNN that were differentiated from NPC in this study. So far, no data on DA treatment of hNN *in vitro* is available. As recently shown, rNN grown on MEAs are well suited for screening large amounts of neurotoxic compounds. This is especially due to their low inter-experimental variability (Frank et al., 2017; Shafer et al., 2019).

To compare the hNN *in vitro* system to developing brains *in vivo*, we performed transcriptome analyses of hiPSC, hiNPC and further differentiated NN at 5, 14 and 28 DIV. Different *in vitro* differentiation stages clearly separate in the PCA analyses showing hiPSC differentiation potential on a global gene expression level. Similar results were published earlier *e.g.* for generating good manufacturing practice grade hiNPC for therapeutic purposes (Rosati et al., 2018) as well as for hiPSC-derived brain organoids (Amiri et al., 2018). The *in vitro-in vivo* comparison relates DEX genes between 0 and 28DIV with DEX genes between 6 and 12 weeks post conception from the previously published data of *in vivo* prefrontal cortex samples (Kang et al., 2011). Of the 2837 DEX genes during early brain development *in vivo*, 868 are also regulated *in vitro* indicating that as expected only a fraction of the neurodevelopmental processes that are regulated in the intact organ take place *in vitro*. However, enriched GO-terms of the *in vitro* cultures reveal presence of well-defined cellular differentiation processes.

5. Summary and conclusion

NN from hiNPC cultured as neurospheres consist of a co-culture of neurons and astrocytes. Synapse-specific proteins, neuronal subtype-specific receptors and enzymes are expressed and respective proteins are present. While GABAR are shown to be functional, glutamate related receptors seem to be absent or lack maturity, which is a limitation of this model. In contrast, at least the NMDAR seems to be functional in rNN that are also responsive to GABA. The neuronal maturation medium CINDA resulted in higher NN activity levels compared to NDM. Formation of NN in this work relied on spontaneous, self-organized hiNPC differentiation, maturation and synapse formation and is therefore highly variable. This is a critical hurdle for pharmacological or toxicological applications. Use of multi-well MEAs compared to single well MEAs seems to improve variability of MEA measurements, but more optimizing work is needed before this system is ready for testing application. Yet in the future GABAergic hNN grown in CINDA medium might be useful as part of an *in vitro* battery for assessing neurotoxicity.

CRediT authorship contribution statement

Laura Nimtz: Conceptualization, Methodology, Investigation, Writing - original draft. **Julia Hartmann:** Investigation, Writing - review & editing. **Julia Tigges:** Supervision, Writing - original draft. **Stefan Masjosthusmann:** Formal analysis, Writing - original draft. **Martin Schmuck:** Software. **Eike Keßel:** Software. **Stephan Theiss:** Software. **Karl Köhrer:** Data curation. **Patrick Petzsch:** Data curation. **James Adjaye:** Resources. **Claudia Wigmann:** Formal analysis. **Dagmar Wieczorek:** Data curation. **Barbara Hildebrandt:** Data curation. **Farina Bendt:** Investigation. **Ulrike Hübenthal:** Investigation. **Gabriele Brockerhoff:** Investigation. **Ellen Fritsche:** Funding acquisition, Supervision, Project administration, Writing - review & editing.

Acknowledgments

This work was supported by the project CERST (Center for Alternatives to Animal Testing) of the Ministry for innovation, science and research of the State of North-Rhine Westphalia, Germany [file number 233-1.08.03.03-121972].

Disclosure of Potential Conflicts of Interest

None.

Supplementary materials

Supplementary material associated with this article can be found, in the online version, at doi:10.1016/j.scr.2020.101761.

References

Alloisio, S., Nobile, M., Novellino, A., 2015. Multiparametric characterisation of neuronal network activity for *in vitro* agrochemical neurotoxicity assessment. Neurotoxicology 48, 152–165. https://doi.org/10.1016/j.neuro.2015.03.013.

Andres, R.H., Ducray, A.D., Schlattner, U., et al., 2008. Functions and effects of creatine in the central nervous system. Brain Res. Bull. 76, 329–343. https://doi.org/10.1016/j.

brainresbull.2008.02.035.
Amiri, A., Coppola, G., Scuderi, S., et al., 2018. Transcriptome and epigenome landscape of human cortical development modeled in organoids. Science 362, 6420. https://doi.org/10.1126/science.aat6720.
Aschner, M., Ceccatelli, S., Daneshian, M., et al., 2017. Reference compounds for alternative test methods to indicate developmental neurotoxicity (DNT) potential of chemicals: example lists and criteria for their selection and use. ALTEX 34, 49–74. https://doi.org/10.14573/altex.1604201.
Bal-Price, A.K., Sunol, C., Weiss, D.G., et al., 2008. Application of *in vitro* neurotoxicity testing for regulatory purposes: symposium iii summary and research needs. Neurotoxicology 29, 520–531. https://doi.org/10.1016/j.neuro.2008.02.008.
Baumann, J., Gassmann, K., Fritsche, E., 2014. Comparative human and rat "Neurosphere assay" for developmental neurotoxicity testing. In: Costa, L.G., Davila, J.C., Lawrence, D.A., Reed, D.J. (Eds.), Current Protocols in Toxicology. John Wiley & Sons.
Baumann, J., Gassmann, K., Masjosthusmann, S., et al., 2016. Comparative human and rat neurospheres reveal species differences in chemical effects on neurodevelopmental key events. Arch. Toxicol. 90, 1415–1427. https://doi.org/10.1007/s00204-015-1568-8.
Belinsky, G.S., Sirois, C.L., Rich, M.T., et al., 2013. Dopamine receptors in human embryonic stem cell neurodifferentiation. Stem Cells Dev. 22, 1522–1540. https://doi.org/10.1089/scd.2012.0150.
Brown, J.P., Hall, D., Frank, C.L., et al., 2016. Editor's highlight: evaluation of a microelectrode array-based assay for neural network ontogeny using training set chemicals. Toxicol. Sci.: Off. J. Soc. Toxicol. 154, 126–139. https://doi.org/10.1093/toxsci/kfw147.
Chandrasekaran, A., Ponnambalam, G., Kaur, C., 2004. Domoic acid-induced neurotoxicity in the hippocampus of adult rats. Neurotox. Res. 6, 105–117. https://doi.org/10.1007/bf03033213.
Clarke, L.E., Barres, B.A., 2013. Emerging roles of astrocytes in neural circuit development. Nat. Rev. Neurosci. 14, 311–321. https://doi.org/10.1038/nrn3484.
Coecke, S., Eskes, C., Gartlon, J., et al., 2006. The value of alternative testing for neurotoxicity in the context of regulatory needs. Environ. Toxicol. Pharmacol. 21, 153–167. https://doi.org/10.1016/j.etap.2005.07.006.
Costa, L.G., Giordano, G., Guizzetti, M., et al., 2008. Neurotoxicity of pesticides: a brief review. Front. Biosci. 13, 1240–1249. https://doi.org/10.2741/2758.
Cotterill, E., Charlesworth, P., Thomas, C.W., et al., 2016. A comparison of computational methods for detecting bursts in neuronal spike trains and their application to human stem cell-derived neuronal networks. J. Neurophysiol. 116, 306–321. https://doi.org/10.1152/jn.00093.2016.
Dach, K., Bendt, F., Huebenthal, U., et al., 2017. BDE-99 impairs differentiation of human and mouse NPCs into the oligodendroglial lineage by species-specific modes of action. Sci. Rep. 7. https://doi.org/10.1038/srep44861.
Deng, L., Yao, J., Fang, C., et al., 2007. Sequential postsynaptic maturation governs the temporal order of GABAergic and glutamatergic synaptogenesis in rat embryonic cultures. J. Neurosci. 27, 10860–10869. https://doi.org/10.1523/JNEUROSCI.2744-07.2007.
Dutta, A., Gautam, R., Chatterjee, S., et al., 2015. Ascorbate protects neurons against oxidative stress: a Raman microspectroscopic study. ACS Chem. Neurosci. 6, 1794–1801. https://doi.org/10.1021/acschemneuro.5b00106.
EPA, U.S.1998, Health Effects Guidelines OPPTS 870.6200, Neurotoxicity Screening Battery, vol. EPA 71.
Frank, C.L., Brown, J.P., Wallace, K., et al., 2017. From the cover: developmental neurotoxicants disrupt activity in cortical networks on microelectrode arrays: results of screening 86 compounds during neural network formation. Toxicol. Sci.: Off. J. Soc. Toxicol. 160, 121–135. https://doi.org/10.1093/toxsci/kfx169.
Fritsche, E., Gassmann, K., Schreiber, T., 2011. Neurospheres as a model for developmental neurotoxicity testing. Methods Molec. Biol. 758, 99–114. https://doi.org/10.1007/978-1-61779-170-3_7.
Fukushima, K., Miura, Y., Sawada, K., et al., 2016. Establishment of a human neuronal network assessment system by using a human neuron/astrocyte co-culture derived from fetal neural stem/progenitor cells. J. Biomol. Screen. 21, 54–64. https://doi.org/10.1177/1087057115610055.
Gassmann, K., Abel, J., Bothe, H., Haarmann-Stemmann, T., Merk, H.F., Quasthoff, K.N., Rockel, T.D., Schreiber, T., Fritsche, E., 2010. Species-specific differential ahr expression protects human neural progenitor cells against developmental neurotoxicity of PAHs. Environ. Health Perspect. 118, 1571–1577. https://doi.org/10.1289/ehp.0901545.
Gegelashvili, G., Schousboe, A., 1998. Cellular distribution and kinetic properties of high-affinity glutamate transporters. Brain Res. Bull. 45, 233–238. https://doi.org/10.1016/s0361-9230(97)00417-6.
Hofrichter, M., Nimtz, L., Tigges, J., Kabiri, Y., et al., 2017. Comparative performance analysis of human iPSC-derived and primary neural progenitor cells (NPC) grown as neurospheres *in vitro*. Stem Cell Res. 25, 72–82. https://doi.org/10.1016/j.scr.2017.10.013.
Hogberg, H.T., Sobanski, T., Novellino, A., et al., 2011. Application of micro-electrode arrays (MEAs) as an emerging technology for developmental neurotoxicity: evaluation of domoic acid-induced effects in primary cultures of rat cortical neurons. Neurotoxicology 32, 158–168. https://doi.org/10.1016/j.neuro.2010.10.007.
Hyvärinen, Tanja, Hyysalo, Anu, Kapucu Emre, Fikret, et al., 2019. Functional characterization of human pluripotent stem cell-derived cortical networks differentiated on laminin-521 substrate: comparison to rat cortical cultures. Nature Scientific Reports. https://doi.org/10.1038/s41598-019-53647-8.
Izsak, J., Seth, H., Andersson, M., et al., 2019. Robust generation of person-specific, synchronously active neuronal networks using purely isogenic human iPSC-3D neural aggregate cultures. Front. Neurosci. 13 (351). https://doi.org/10.3389/fnins.2019.00351.
Jennings, P., 2015. "The future of *in vitro* toxicology. Toxicol. In Vitro 29, 1217–1221. https://doi.org/10.1016/j.tiv.2014.08.011.
Johnstone, A.F., Gross, G.W., Weiss, D.G., et al., 2010. Microelectrode arrays: a physiologically based neurotoxicity testing platform for the 21st century. Neurotoxicology 31, 331–350. https://doi.org/10.1016/j.neuro.2010.04.001.
Kang, H.J., Kawasawa, Y.I., Cheng, F., et al., 2011. Spatio-temporal transcriptome of the human brain. Nature 478, 483–489. https://doi.org/10.1038/nature10523.
Kao, C.F., Chuang, C.Y., Chen, C.H., et al., 2008. Human pluripotent stem cells: current status and future perspectives. Chin. J. Physiol. 51, 214–225.
Kasteel, E.E., Westerink, R.H., 2017. Comparison of the acute inhibitory effects of Tetrodotoxin (TTX) in rat and human neuronal networks for risk assessment purposes. Toxicol. Lett. 270, 12–16. https://doi.org/10.1016/j.toxlet.2017.02.014.
Leipzig, N.D., Xu, C., Zahir, T., Shoichet, M.S., 2010. Functional immobilization of interferon-gamma induces neuronal differentiation of neural stem cells. J. Biomed. Mater. Res. A 93, 625–633. https://doi.org/10.1002/jbm.a.32573.
Leist, M., Hartung, T., 2013. Inflammatory findings on species extrapolations: humans are definitely no 70-kg mice. Arch. Toxicol. 87, 563–567. https://doi.org/10.1007/s00204-013-1038-0.
Lisman, J.E., 1997. Bursts as a unit of neural information: making unreliable synapses reliable. Trends Neurosci. 20, 38–43. https://doi.org/10.1016/S0166-2236(96)10070-9.
Liu, H., Zhang, S.C., 2011. Specification of neuronal and glial subtypes from human pluripotent stem cells. Cell. Molec. Life Sci. 68, 3995–4008. https://doi.org/10.1007/s00018-011-0770-y.
Lujan, R., Shigemoto, R., Lopez-Bendito, G., 2005. Glutamate and GABA receptor signalling in the developing brain. Neuroscience 130, 567–580. https://doi.org/10.1016/j.neuroscience.2004.09.042.
Mack, C.M., Lin, B.J., Turner, J.D., et al., 2014. Burst and principal components analyses of MEA data for 16 chemicals describe at least three effects classes. Neurotoxicology 40, 75–85. https://doi.org/10.1016/j.neuro.2013.11.008.
Maeda, E., Robinson, H.P., Kawana, A., 1995. The mechanisms of generation and propagation of synchronized bursting in developing networks of cortical neurons. J. Neurosci. 15, 6834–6845. https://doi.org/10.1523/JNEUROSCI.15-10-06834.1995.
Magdalini, S., Munn, S., Bal-Price, A., 2019. AOP: 48. Binding of Agonists to Ionotropic Glutamate Receptors in Adult Brain Causes Excitotoxicity that Mediates Neuronal Cell Death, Contributing to Learning and Memory Impairment. AOPwiki.org.
Masjosthusmann, S., Barenys, M., Elgamal, M., et al. 2018a, Literature Review and Appraisal On Alternative Neurotoxicity Testing Methods, External Scientific Report, 10.2903/sp.efsa.2018.EN-1410.
Masjostusmann, S., Becker, D., Petzuch, B., et al., 2018b. A transcriptome comparison of time-matched developing human, mouse and rat neural progenitor cells reveals human uniqueness. Toxicol. Appl. Pharmacol. 354, 40–55. https://doi.org/10.1016/j.taap.2018.05.009.
Matthews, R.A., 2008. Medical progress depends on animal models – doesn't it? J. R. Soc. Med. 101, 95–98. https://doi.org/10.1258/jrsm.2007.070164.
Mayer, M., Arrizabalaga, O., Lieb, F., et al., 2018. Electrophysiological investigation of human embryonic stem cell derived neurospheres using a novel spike detection algorithm. Biosens. Bioelectron. 100, 462–468. https://doi.org/10.1016/j.bios.2017.09.034.
McConnell, E.R., McClain, M.A., Ross, J., et al., 2012. Evaluation of multi-well microelectrode arrays for neurotoxicity screening using a chemical training set. Neurotoxicology 33, 1048–1057. https://doi.org/10.1016/j.neuro.2012.05.001.
Michalczyk, K., Ziman, M., 2005. Nestin structure and predicted function in cellular cytoskeletal organisation. Histol. Histopathol. 20, 665–671. https://doi.org/10.14670/HH-20.665.
Molofsky, A.V., Deneen, B., 2015. Astrocyte development: a guide for the perplexed. Glia 63, 1320–1329. https://doi.org/10.1002/glia.22836.
Molofsky, A.V., Krencik, R., Ullian, E.M., et al., 2012. Astrocytes and disease: a neurodevelopmental perspective. Genes Dev. 26, 891–907. https://doi.org/10.1101/gad.188326.112.
Napoli, Alessandro, Obeid, Iyad, 2016. Comparative Analysis of Human and Rodent Brain Primary Neuronal Culture Spontaneous Activity Using Micro-Electrode Array Technology. Journal of Cellular Biochemistry https://doi.org/10.1002/jcb.25312.
Nat, R., Nilbratt, M., Narkilahti, S., et al., 2007. Neurogenic neuroepithelial and radial glial cells generated from six human embryonic stem cell lines in serum-free suspension and adherent cultures. Glia 55, 385–399. https://doi.org/10.1002/glia.20463.
Oberheim, N.A., Wang, X., Goldman, S., et al., 2006. Astrocytic complexity distinguishes the human brain. Trends Neurosci. 29, 547–553. https://doi.org/10.1016/j.tins.2006.08.004.
Odawara, A., Katoh, H., Matsuda, N., et al., 2016. Physiological maturation and drug responses of human induced pluripotent stem cell-derived cortical neuronal networks in long-term culture. Sci. Rep. 6, 26181. https://doi.org/10.1038/srep26181.
Odawara, A., Saitoh, Y., Alhebshi, A.H., et al., 2014. Long-term electrophysiological activity and pharmacological response of a human induced pluripotent stem cell-derived neuron and astrocyte co-culture. Biochem. Biophys. Res. Commun. 443, 1176–1181. https://doi.org/10.1016/j.bbrc.2013.12.142.
OECD, Test No. 424: Neurotoxicity Study in Rodents, 1997.
Paavilainen, T., Pelkonen, A., Makinen, M.E., et al., 2018. Effect of prolonged differentiation on functional maturation of human pluripotent stem cell-derived neuronal cultures. Stem Cell Res. 27, 151–161. https://doi.org/10.1016/j.scr.2018.01.018.
Pistollato, F., Canovas-Jorda, D., Zagoura, D., et al., 2017. Nrf2 pathway activation upon rotenone treatment in human iPSC-derived neural stem cells undergoing differentiation towards neurons and astrocytes. Neurochem. Int. 108, 457–471. https://doi.org/10.1016/j.neuint.2017.06.006.

Pistollato, F., Louisse, J., Scelfo, B., et al., 2014. Development of a pluripotent stem cell derived neuronal model to identify chemically induced pathway perturbations in relation to neurotoxicity: effects of CREB pathway inhibition. Toxicol. Appl. Pharmacol. 280, 378–388. https://doi.org/10.1016/j.taap.2014.08.007.

Robinton, D.A., Daley, G.Q., 2012. The promise of induced pluripotent stem cells in research and therapy. Nature 41, 295–305. https://doi.org/10.1038/nature10761.

Rosati, J., Ferrari, D., Altieri, F., et al., 2018. Establishment of stable iPS-derived human neural stem cell lines suitable for cell therapies. Cell Death Dis. 9 (10), 937.

Russell Jr., W.F., Kass, I., Heaton, A.D., et al., 1959. Combined drug treatment of tuberculosis. III. Clinical application of the principles of appropriate and adequate chemotherapy to the treatment of pulmonary tuberculosis. J. Clin. Invest. 38, 1366–1375. https://doi.org/10.1172/JCI103912.

Seidel, D., Jahnke, H.G., Englich, B., et al., 2017. *In vitro* field potential monitoring on a multi-microelectrode array for the electrophysiological long-term screening of neural stem cell maturation. Analyst 142, 1929–1937. https://doi.org/10.1039/c6an02713j.

Semple, B.D., Blomgren, K., Gimlin, K., et al., 2013. Brain development in rodents and humans: identifying benchmarks of maturation and vulnerability to injury across species. Prog. Neurobiol. 106–107, 1–16. https://doi.org/10.1016/j.pneurobio.2013.04.001.

Shafer, T.J., Brown, J.P., Lynch, B., et al., 2019. Evaluation of chemical effects on network formation in cortical neurons grown on microelectrode arrays. Toxicol. Sci.: Off. J. Soc. Toxicol. 169, 436–455. https://doi.org/10.1093/toxsci/kfz052.

Shimba, K., Sakai, K., Iida, S., et al., 2019. Long-term developmental process of the human cortex revealed *in vitro* by axon-targeted recording using a microtunnel-augmented microelectrode array. IEEE Trans. Biomed. Eng. 66, 2538–2545. https://doi.org/10.1109/TBME.2019.2891310.

Singh, V.K., Kalsan, M., Kumar, N., et al., 2015. Induced pluripotent stem cells: applications in regenerative medicine, disease modeling, and drug discovery. Front. Cell Dev. Biol. 3 (2). https://doi.org/10.3389/fcell.2015.00002.

Suter-Dick, L., Alves, P.M., Blaauboer, B.J., et al., 2015. Stem cell-derived systems in toxicology assessment. Stem Cells Dev. 24, 1284–1296. https://doi.org/10.1089/scd.2014.0540.

Takahashi, K., Okita, K., Nakagawa, M., et al., 2007. Induction of pluripotent stem cells from fibroblast cultures. Nat. Protoc. 2, 3081–3089. https://doi.org/10.1038/nprot.2007.418.

Tang, X., Zhou, L., Wagner, A.M., et al., 2013. Astroglial cells regulate the developmental timeline of human neurons differentiated from induced pluripotent stem cells. Stem Cell Res. 11 (2), 743–757. https://doi.org/10.1016/j.scr.2013.05.002.

Tjarnlund-Wolf, A., Hultman, K., Blomstrand, F., et al., 2014. Species-Specific regulation of t-PA and PAI-1 gene expression in human and rat astrocytes. Gene Regul. Syst. Biol. 8, 113–118. https://doi.org/10.4137/GRSB.S13387.

Toivonen, S., Ojala, M., Hyysalo, A., et al., 2013. Comparative analysis of targeted differentiation of human induced pluripotent stem cells (hiPSCs) and human embryonic stem cells reveals variability associated with incomplete transgene silencing in retrovirally derived hiPSC lines. Stem Cells Transl. Med. 2, 83–93. https://doi.org/10.5966/sctm.2012-0047.

Tukker, A.M., Wijnolts, F.M.J., de Groot, A., et al., 2018. Human iPSC-derived neuronal models for *in vitro* neurotoxicity assessment. Neurotoxicology 67, 215–225. https://doi.org/10.1016/j.neuro.2018.06.007.

Tukker, A.M., de Groot, M.W., Wijnolts, F.M., et al., 2016. Is the time right for *in vitro* neurotoxicity testing using human iPSC-derived neurons? ALTEX 33, 261–271. https://doi.org/10.14573/altex.1510091.

Valdivia, P., Martin, M., LeFew, W.R., et al., 2014. Multi-well microelectrode array recordings detect neuroactivity of ToxCast compounds. Neurotoxicology 44, 204–217. https://doi.org/10.1016/j.neuro.2014.06.012.

Vassallo, A., Chiappalone, M., De Camargos Lopes, R., et al., 2017. A multi-laboratory evaluation of microelectrode array-based measurements of neural network activity for acute neurotoxicity testing. Neurotoxicology 60, 280–292. https://doi.org/10.1016/j.neuro.2016.03.019.

Wagenaar A., Daniel, Pine, Jerome, Potter M, Steve, 2006. An extremely rich repertoire of bursting patterns during the development of cortical cultures. BMC Neuroscience 7 (11) https://doi.org/10.1186/1471-2202-7-11.

Wallace, K., Strickland, J.D., Valdivia, P., et al., 2015. A multiplexed assay for determination of neurotoxicant effects on spontaneous network activity and viability from microelectrode arrays. Neurotoxicology 49, 79–85. https://doi.org/10.1016/j.neuro.2015.05.007.

Walls, A.B., Waagepetersen, H.S., Bak, L.K., et al., 2015. The glutamine-glutamate/GABA cycle: function, regional differences in glutamate and GABA production and effects of interference with GABA metabolism. Neurochem. Res. 40, 402–409. https://doi.org/10.1007/s11064-014-1473-1.

Walter, K.M., Dach, K., Hayakawa, K., et al., 2019. Ontogenetic expression of thyroid hormone signaling genes: an *in vitro* and *in vivo* species comparison. PLoS ONE 14, e0221230. https://doi.org/10.1371/journal.pone.0221230.

Wang, Y., Adjaye, J., 2011. A cyclic amp analog, 8-Br-cAMP, enhances the induction of pluripotency in human fibroblast cells. Stem Cell Rev. Rep. 7, 331–341. https://doi.org/10.1007/s12015-010-9209-3.

Watanabe, K.H., Andersen, M.E., Basu, N., et al., 2011. Defining and modeling known adverse outcome pathways: domoic acid and neuronal signaling as a case study. Environ. Toxicol. Chem. 30, 9–21. https://doi.org/10.1002/etc.373.

Xiang, G., Pan, L., Huang, L., et al., 2007. Microelectrode array-based system for neuropharmacological applications with cortical neurons cultured *in vitro*. Biosens. Bioelectron. 22, 2478–2484. https://doi.org/10.1016/j.bios.2006.09.026.

Yuan, S.H., Martin, J., Elia, J., et al., 2011. Cell-surface marker signatures for the isolation of neural stem cells, glia and neurons derived from human pluripotent stem cells. PLoS ONE 6, e17540. https://doi.org/10.1371/journal.pone.0017540.

Zagoura, D., Canovas-Jorda, D., Pistollato, F., et al., 2017. Evaluation of the rotenone-induced activation of the Nrf2 pathway in a neuronal model derived from human induced pluripotent stem cells. Neurochem. Int. 106, 62–73. https://doi.org/10.1016/j.neuint.2016.09.004.

Zhang, Y., Pak, C., Han, Y., et al., 2013. Rapid single-step induction of functional neurons from human pluripotent stem cells. Neuron 78, 785–798. https://doi.org/10.1016/j.neuron.2013.05.029.

Zhu, G., Sun, C., Liu, W., 2012. Effects of neurotrophin-3 on the differentiation of neural stem cells into neurons and oligodendrocytes. Neural Regen. Res. 7, 1483–1487. https://doi.org/10.3969/j.issn.1673-5374.2012.19.006.

Zuang, V., Casati, S., Aschberger, K., et al., 2018. Standardisation of defined approaches for skin sensitisation testing to support regulatory use and international adoption: position of the international cooperation on alternative test methods. Arch. Toxicol. 92, 611–617. https://doi.org/10.1007/s00204-017-2097-4.

Zuang, V., Barroso, J., Belz, S., et al., EURL ecvam status report on the development, validation and regulatory acceptance of alternative methods and approaches in Publications Office of the European Union, 2017, 10.2760/818599.